Hebron University Research Journal-A (Natural Sciences) - (مجلة جامعة الخليل للبحوث- أ (العلوم الطبيعيه)

Volume 9 | Issue 1 Article 5

2020

Compressed TH M-Ary PPM Technique for Improved Performance of UWB Radio

adnan Arar
Hebron University, adnana@hebron.edu

Ahmed MASRI
Jyväskylä, Finland, r.journal@hebron.edu

Yousef DAMA
An-Najah National, sanad@hebron.edu

Hebron University Research Journal(A)
Vol.(9), pp.(87-109), 2020

H.U.R.J. is available online at
http://www.hebron.edu/journal

Compressed TH M-Ary PPM Technique for Improved Performance of UWB Radio

Adnan ARAR[1], Ahmed MASRI[2,3], and Yousef DAMA[3]

[1]College of Science and Technology, Hebron University, Hebron, Palestine

[2]Magister Solutions - Jyväskylä, Finland

[3]Faculty of Engineering and Information Technology, An-Najah National University, Nablus, Palestine

Corresponding author: adnana@hebron.edu

Received: (22/5/2020), Accepted: (24/9/2020)

Abstract

This study presents the performance of Ultra-Wideband (UWB) technology under an interference dominated scenario and realistic channel model. The study also proposes a modified version of Time Hopping (TH) M-Ary Pulse Position Modulation (PPM) for UWB to save communication resources and improve quality of service (QoS). Compared with the conventional TH M-Ary PPM technique, the proposed Compressed M-Ary PPM (CTH M-Ary PPM) technique is to adopt fixed symbol duration (T_s) for all M PPM modulation levels, which results in reducing the number of TH chips (G), improving the SINR at the pulse level and reducing the overall time required to complete the transmission of the same amount of data from any user. As a consequence, lowering the overall probability of users' collisions, and so, reducing the chance of interference to occur from the beginning on the pulse level. Detailed channel model and Signal-to-Interference-pulse-Noise-Ratio (SINR) derivations are presented. The designed Simulation results confirm that the new proposed scheme enhances

transmission quality in terms of Symbol Error Probability (SEP) as a comparison with the conventional TH M-Ary PPM technique.

Keywords

M-Ary Pulse Position Modulation; Time Hopping; Symbol Error Probability; Ultra Wideband

الملخّص:

تُقدّم هذه الدّراسة أداء تقنية النّطاق فائق العرض (UWB) في ظلّ سيناريو يُهيمن عليه التّداخل ونموذج القناة الواقعيّة، وتقترح إصدارًا مُعدّلًا للقفز الزّمنيّ في تعديل موقع النبضة (TH M-Ary PPM) للنّطاق فائق العرض من أجل توفير موارد الاتّصال، وتحسين جَوْدة الخدمة (QoS)، مقارنةً بتقنية (TH M-Ary PPM) التّقليديّة. تتجلّى الفكرة من وراء تقنية القفز الزّمنيّ المضغوطة في تعديل موقع النبضة (CTH M-Ary PPM) باعتماد مدّةٍ ثابتةٍ للرّمز (T_s) لجميع مستويات تعديل موقع النبضة ($M-PPM$)، ممّا يفضي إلى: تقليل عدد رقائق القفز الزّمنيّ (G)؛ تحسين نسبة الإشارة إلى التّداخل والضّوضاء على مستوى النّبضات؛ تقليل الوقت الإجماليّ المطلوب لإكمال نقل كمّيّة البيانات نفسها من أيّ مُستخدم؛ بحيث ينجمُ عن ذلك تقليل احتمال التّصادم بين المستخدمين، وبالتالي تقليل فرصة حدوث التّداخل من البداية على مستوى النّبضات. تـمّ عرض نموذج قناة مُفصّل، ومشتقات نسبة الإشارة إلى التّداخل والضّوضاء (SINR)، كما تـمّ استخدام احتمال خطأ الرّمز (SEP) باعباره مقياسًا للأداء. وتُؤكّد نتائج المحاكاة المُصمّمة أنّ المُخطّط المقترح الجديد يُعزّز جَوْدة الإرسال من حيثُ احتمال خطأ الرّمز بالمقارنة مع التّقنية التّقليديّة.

1. Introduction

"Pulse-based Ultra-Wide Band (UWB) transmission is the emerging opportunity for modern wireless communication in the microwave and millimeter-wave (mm-wave) frequency ranges" (JAIN. *et al.*, 2017). UWB technology is considered a primary candidate in upcoming standards for the physical layer of wireless personal area networks to provide reliable high-speed data transmission at short range in severe multipath conditions. It exhibits robust Multiple Access (MA) performance with little interference to other communication systems sharing the same bandwidth. For communication devices, the Federal Communications Commission (FCC) has

assigned different emission limits for indoor and outdoor UWB devices as depicted in Figure 1 (Nekoogar. *et al.,* 2005; FCC., 2002; Zhang. *et al.*, 2009). According to the FCC regulations, the maximum Equivalent Isotropically Radiated Power (EIRP) in any direction should not exceed -41.3 dBm. Thus, it offers a promising solution to the scarcity of RF spectrum by allowing new services to coexist concurrently with other radio systems with minimal and avoiding the expensive spectrum licensing fees that providers of all other radio services must pay (FCC., 2002).

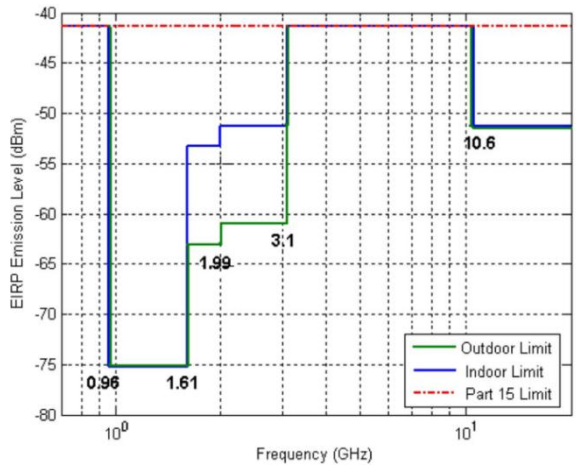

Fig. 1. FCC emissions limits

The fundamental characteristic of UWB is its extremely large bandwidth, which is required since very narrow pulses of appropriate shape and sub-nanosecond duration are used by the transmitted signal (Masri. *et al.*, 2012). One of the most widely studied UWB schemes employs Pulse Position Modulation (PPM) combined with Time-Hopping (TH) as its multiple access technique. The UWB pulses are time-hopped within a fixed time window, or frame, and each transmitted symbol is spread over several pulses in order to facilitate multiple user access (Kokkalis. *et al.*, 2006).

Several literature works have been investigating the design and implementation of TH M-Ary PPM for UWB radio technology (Zhang. *et al.*, 2009; Kokkalis. *et al.*, 2008; Wang. *et al.*, 2014; Di Benedetto. *et al.*, 2005; Shen. *et al.*, 2011).

Authors in (Kokkalis. *et al.*, 2008), derived an expression for the capacity of a TH-UWB system in the presence of narrowband interference. While in (Wang. *et al.*, 2014), "the multiple access performance of the single-user correlation receiver for ultra wideband time hopping bipolar modulation impulse radio was analyzed in terms of the signal-noise ratio (SNR) and the bit error rate (BER) from the spectrum point of view". Moreover, MAC layer design was carried out in (Di Benedetto. *et al.*, 2005), where authors revisited the technique of $(UWB)^2$ MAC protocol (Maria. *et al.*, 2005) in view of its application to IEEE 802.15.4a, for both centralized and distributed network topologies. In (Shen. *et al.*, 2011), a new TH/Direct sequence UWB system was proposed employing the whole frame to carry out TH and M-Ary bi-orthogonal PPM. Their simulation results show that the proposed TH/DS system outperforms the current scheme. Meanwhile, in (Masri. *et al.*, 2010) authors were using UWB radio technology as part of cognitive radio to solve the common control channel problem, "over which nodes will be able to discover each other and exchange control information for establishing a communication link". In another work (Bai. *et al.*, 2006), the authors proposed a modified M-Ary modulation by combining signal partitioning with pulse position modulation, in which they investigated three different signal partitioning techniques, namely; Ungreboeck Partitioning (UP), Block Partitioning (BP) and Mixed Partitioning (MP). Moreover, they evaluated their system over a simple Additive White Gaussian Noise (AWGN) channel with perfect time synchronization and correlation receiver.

This paper, on one side, investigates the performance of UWB radio technology over interference dominated system and realistic channel model. On the other side, it proposes a modified version of the conventional Impulse Response (IR) TH M-Ary PPM UWB radio technology. In addition, a detailed channel model and SINR derivations are provided. The performance of the modified version is tested by carrying out extensive simulations over realistic channel model. Moreover, a comparison to the conventional TH M-Ary PPM is presented.

This paper is organized as follows: System Model with detailed Transmission Technique and propagation model are described in subsections 2.1 and 2.2, respectively. The conventional M-Ary TH PPM and the derivation of the SINR are detailed in subsections 2.3 and 2.4, respectively. In Section 3, the proposed Compressed TH M-Ary PPM is presented. Moreover, a complete performance evaluation is given in Section 4, with a full description of the reference scenario in use with results discussion. Finally, conclusions are drawn in Section 5.

2. System Model

2.1 Transmission Technique

Starting from the model derived in (Molisch. *et al.*, 2006), a physical channel which consists of a power delay profile is adopted, and the parameter values for CM9 (farm environment) are used. This model will be used later to compute the SINR and SEP. Assume N users transmitting asynchronously, the TH M-Ary PPM signal of the n^{th} user can be modeled as (Lovelace. *et al.*, 2002)

$$s^n(t) = \sqrt{E_p^n} \sum_{r=-\infty}^{\infty} p\left(t - rT_f - c_r^n T_c - \delta d_v^n\right) \qquad (1)$$

where $p(t)$ is a reference pulse of duration T_m, $E_p^n = E_{max} = T_m . B. 10^{(-41.3/10)}$ mW is the energy transmitted for each pulse from the n^{th} user, and $(1 \leq n \leq N)$, $T_f = T_s/N_p$ is the frame duration and T_c is the chip duration. $G = T_f/T_c$ is the number of time-hopping slots and the n^{th} user's hopping sequence c_r^n is a sequence of integers in $[0, G-1]$, d_v^n is the transmitted symbol $0 \leq d_v^n \leq M - 1$ of the n^{th} user, and $v = (r/N_p)$, where v is the largest integer y with $y \leq v$ and δ time shift difference between two subsequent PPM signals, $\delta \geq T_m . N_p$ Pulses/symbol are transmitted providing a symbol rate of $R = 1/(N_p T_f)$ and energy per symbol $E_s = N_p E_p$.

The receiver performs a correlation between the received signal and the reference pulse $p(t)$. When such a receiver operates in an AWGN channel, the symbol error probability of the 2PPM is given by (Durisi. *et al.*, 2003)

$$P(e) = \frac{1}{2} erfc \sqrt{\frac{E_s}{2N_0}\left(1 - \gamma(\delta)\right)} \qquad (2)$$

where: $\gamma(\delta)$ is the pulse autocorrelation function, and $N_0 = K_B T F L_M$ is the one-sided Power Spectral Density (PSD) of the AWGN. K_B is the Boltzmann constant, and T is the equivalent temperature.

In order to avoid making precise assumptions about the UWB pulse shape, δ is assumed to be zero. The received signal can be expressed as

$$R(t) = \sum_{n=1}^{N} s^{(n)}(t) + N(t) \qquad (3)$$

where $N(t)$ is the AWGN waveform with one-sided PSD N_0.

It is assumed that the transmitted signal has bandwidth $B = 500$ MHz and transmission PSD that matches the FCC limit for the 3.1 to 10.6 GHz frequency range, equal to −41.3 dBm/MHz (FCC., 2002). In order to keep the overall signal bandwidth constant, the pulse duration (T_m) is set to 2 ns, for any modulation order M. For simplicity, all users are assumed to be within the same transmission range of each other. To evaluate the multi-user interference on the pulse level, it is necessary to define a realistic propagation model. Hence, the model and environments defined are adopted as in (Molisch. *et al.*, 2006). A full description for the proposed propagation model comes in the following subsection.

2.2 Propagation Model

This subsection describes the components of the UWB propagation model, with model parameters listed in Table 1.

Path loss model: Given a generic pair of nodes, ***i*** and ***j***, the path loss is modeled as (Masri. *et al.*, 2012)

$$PL_{dB}(d_{ij}) = PL_0 + 10\eta log_{10}\frac{d_{ij}}{d_0} + SL \qquad (4)$$

where PL_0 is the path loss (in dB) at distance $d_0 = 1$ m, d_{ij} is the Euclidean distance between nodes i and j, η is the path loss exponent, and SL is the log-normal random shadowing loss with zero mean and standard deviation σ_{SL} dB.

The average received power during the transmission of a pulse for a given pair of users at distance d is given by (Masri. *et al.*, 2012)

$$P_{RX,dBm} = P_{TX,dBm} - PL_{dB}(d) \qquad (5)$$

Due to the relatively narrow bandwidth, the frequency dependency of the path loss is neglected which is proposed in (Masri. *et al.*, 2010).

Impulse Response Model: The model of impulse response adopted is that proposed in (Molisch. *et al.*, 2006; Saleh. *et al.*, 1987). Accordingly, the impulse response of the channel consists of L clusters with K rays in each is (Molisch. *et al.*, 2006)

$$h(t) = \sum_{l=0}^{L-1} \sum_{k=0}^{K-1} a_{k,l} e^{j\varphi_{k,l}} \delta\left(t - T_l - \tau_{k,l}\right) \qquad (6)$$

where $a_{k,l}$ is the tap weight of the k^{th} component in the l^{th} cluster delay, $\varphi_{k,l}$ is uniformly distributed in $[0, 2\pi]$, T_l is the l^{th} cluster delay, and $\tau_{k,l}$ is the delay of the k^{th} ray relative to T_l.

Furthermore, it is assumed, as in (Molisch. *et al.*, 2006), that the number of clusters L is a Poisson-distributed random variable with mean $\bar{L}$. A typical channel impulse response is shown in Figure 2.

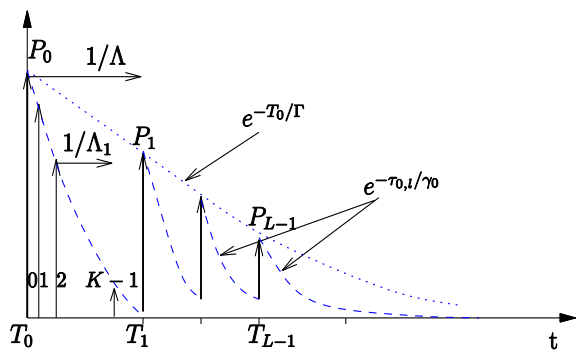

Fig. 2. Typical impulse response of channel consists of L clusters with K rays each, rate Λ is a mixture of (λ_1, λ_2). Adapted from "Common control channel allocation in cognitive radio networks through UWB communication" by Masri, A., Chiasserini, C. F., Casetti, C., & Perotti, A., 2012, Journal of

Communications and Networks. vol.14 ,no. 6, pp. 710–718. Copyright 2012 by KICS.

Table 1: Parameters of the UWB Propagation Model (Molisch. *et al.*, 2006)

Model	**CM9 (Farm environment)**
Path loss at 1meter, PL_0 (dB)	48.96
Path loss exponent, η	1.58
Shadow fading standard deviation, σ_{SL} (dB)	3.96
Mean number of clusters, $\bar{L}$	3.31
Cluster arrival rate, Λ (1/ns)	0.0305
Ray arrival rates, $\lambda_1\lambda_2$ (1/ns)	0.0225
Ray mixture probability, β	1
Cluster energy decay constant, Γ (ns)	56
Ray energy decay constant, γ_0 (ns)	0.92
Cluster energy standard deviation, σ_{CL} (dB)	3
Nakagami m, mean m_0, standard deviation $\hat{m}_0$ (dB)	4, 1, 2.5

The cluster inter-arrival time is exponentially distributed as (Molisch. *et al.*, 2006)

$$p(T_l|T_{l-1}) = \Lambda exp[-\Lambda(T_l - T_{l-1})] \quad (7)$$

where Λ is the cluster arrival rate. The ray inter-arrival times are modeled by a mixed exponential distribution, given by (Molisch. *et al.*, 2006)

$$p(\tau_{k,l}|\tau_{k-1,l}) =$$
$$\beta\lambda_1 exp[-\lambda_1(\tau_{k,l} - \tau_{k-1,l})] + (\beta 1)\lambda_2 exp[-\lambda_2(\tau_{k,l}\tau_{k-1,l})] \quad (8)$$

where λ_1, λ_2 are the ray arrival rates, β is the mixture probability, and $\tau_{0,l} = 0$. The integrated energy of the l^{th} cluster, Ω_1 expressed in dB, is (Molisch. *et al.*, 2006)

$$10\log(\Omega_1) = 10\log(\exp(-T_l/\Gamma)) + M_{cl} \quad (9)$$

where Γ is the energy decay constant and M_{cl} is a zero-mean Gaussian random variable with standard deviation σ_{cl}.

The average power of each ray is (Molisch. *et al.*, 2006)

$$Expectation\left\{\left|a_{k,l}\right|^2\right\} = \Omega_1 exp(\tau_{k,l}/\gamma_0) \quad (10)$$

where γ_0 is a ray's energy decay constant. Based on the required dynamic range, the number of rays per cluster is chosen such that the rays kept within 30 dB at maximum, i.e. the rays with $\exp\left(-\frac{\tau_{k,l}}{\gamma_0}\right) < 0.001$, are neglected.

The small-scale amplitudes $a_{k,l}$ in equation (6) are Nakagami-m distributed as follows

$$f_a(x) = \frac{2}{\Gamma(m)}\left(\frac{m}{\Omega}\right)^m x^{2m-1}\exp\left(-\frac{m}{\Omega}x^2\right) \quad (11)$$

The Nakagami- m parameter is log-normally distributed with mean m_0 and standard deviation $\hat{m}_0$ and Ω is the mean-square value of the amplitude. Finally, all impulse response realizations are scaled such that the sum of the squared amplitude of all rays has unit power on average, so that equation (4) can be used for scaling the channel.

2.3 Conventional M-Ary TH PPM

Figure 3 summarizes the main conventional symbol structure of the IR TH M-Ary PPM system: Every symbol is repeated N_p times within the symbol duration T_s. Where T_s is subdivided into T_s/N_p frames, each with duration of T_f. Furthermore, each frame duration is subdivided into a number of TH chips with duration of T_c. Finally, a pulse representing the symbol value of duration T_m will fall within one of those chip durations randomly.

As shown in Figure 3, each transmission frame consists of G chip intervals with duration $T_c = MT_m$, where T_m is the pulse duration and M is the number of

symbols of the M − Ary PPM modulation scheme. Based on this definition, the SINR is derived based on the channel model described above.

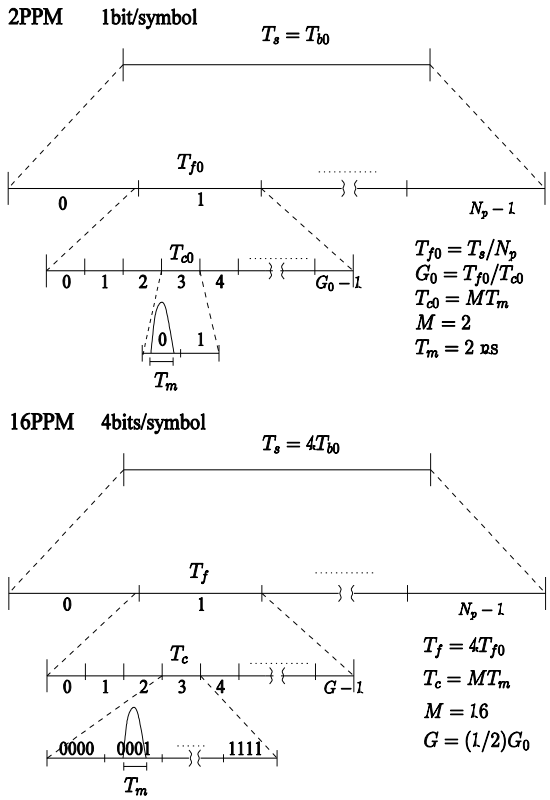

Fig. 3. Symbol structure for the conventional IR TH 2-PPM and 16-PPM modulation. Adapted from "Common control channel allocation in cognitive radio networks through UWB communication" by Masri, A., Chiasserini, C. F., Casetti, C., & Perotti, A., 2012, Journal of Communications and Networks. vol.14 ,no. 6, pp. 710–718. Copyright 2012 by KICS.

2.4 Computation of the SINR

In this subsection, a detailed derivation for the SINR is carried out. In order to obtain a realistic evaluation of the SINR, the power-delay profile is discretized according to the UWB TH PPM scheme, assuming that the receiver consists of a single-correlate matched to the UWB pulse and locked to the highest power ray.

Time hopping codes are of two types; one holds the common TH codes for all users and is used toward establishing the first handshakes, while the other, holds the distinct TH codes, which are used to reduce interference with nearby transmissions in the subsequent communications after the first handshake is established.

Focusing on the interference part of the SINR, it is found that there are two sources of interference: a) from other users who may use the same hopping code (common codes) as the desired user or distinct hopping codes, and b) from some of the desired user's own rays due to multipath. Users with the common hopping code have a random shift which is the same for the whole packet transmission, while for users with distinct hopping codes the delay profile is shifted randomly for each frame. As a consequence, interference occurs when one or more rays of interfering users, including transmissions from earlier frames of the desired user's own frames, falls or fall within the same chip interval as the useful transmission.

Let us denote the propagation delays of the rays between the transmitting user of interest i and receiving user of interest j as $(\tau_{0,0}^{(i,j)}, \dots, \tau_{K-1,L-1}^{(i,j)})$. The strongest ray $\tau_{k_s,l_s}^{(i,j)}$, which is not necessarily $\tau_{0,0}^{(i,j)}$, contributes to the useful received symbol energy as $E_r = E_s \,.\, P_{k_s,l_s}^{(i,j)}$, where $P_{k_s,l_s}^{(i,j)} = 10^{-PL_{dB}(d_{ij})/10} . a_{k_s,l_s}^{(i,j)^2}$.

If an interfering user belongs to a set of users $n \in \mathcal{J}_c$, where $\mathcal{J}_c$ is the set of users using a common hopping sequence, the delays $\tau_{k,l}^{(n,j)}$ are shifted by a random variable $\Delta\tau^{(n,j)} = \Delta\tau_c^{(n,j)}$, which is uniformly distributed in $[0, T_f]$, and constant in each frame for the whole packet transmission. For an interfering user $n \in \mathcal{J}_D$, where $\mathcal{J}_D$ is the set of users with distinct hopping sequence, the propagation delays are shifted by $\Delta\tau_f^{(n,j)} = \Delta\tau_{D,0}^{(n,j)} + \Delta\check{\tau}_{D,f}^{(n,j)}$, where $\Delta\tau_{D,0}^{(n,j)}$ is a random uniformly $[0, T_f]$ distributed offset due to unsynchronized transmission and

$\Delta\check{\tau}_{D,f}^{(n,j)} \in \{0,1,\dots,G-1\}$ is a discrete random variable, which is different for each frame f due to the hopping pattern.

The amount of interfering energy per symbol is approximated by evaluating the amount of energy conveyed by propagation rays that fall within the same chip interval as the useful transmission (including earlier frames) of the user i itself and the interfering users n $\in \{\mathcal{I}_C, \mathcal{I}_D\}$. This energy is hence given by

$$E_I = E_p^n . \sum_{f=0}^{N_p-1} \sum_{n=1}^{N} \sum_{k,l \in \mathcal{I}_f^{(n,j)}} P_{k,l}^{(n,j)} \qquad (12)$$

where $\mathcal{I}_f^{(n,j)}$ denotes the set of interfering ray indexes for f[th] frame of the n[th] user. Interfering ray indexes can be determined by first discretizing all the ray delays into the chip intervals as

$$\check{\tau}_{k,l,f}^{(n,j)} = \left\lfloor \frac{\tau_{k,l,f}^{(n,j)} + \Delta\tau_f^{(n,j)}}{T_c} \right\rfloor \qquad (13)$$

The SINR for the transmission from user i to user j is

$$SINR^{(i,j)} = \frac{E_r}{E_I + E_N} \qquad (14)$$

For each symbol, E_N represents the noise energy, given by

$$E_N = N_0 . \underbrace{B.T_p}_{} . N_p = K_B T F . N_p \qquad (15)$$

where $B.T_p = 1$.

Using a single-correlate receiver reduces the power of the useful signal as some rays constitute self-interference, as can be seen from the formula for the SINR. Using the power delay profiles in the computation of the interference power provides a correct estimate of this power.

Now, let us consider the bit error probability (BEP) for the transmission of the q[th] bit from user i to user j, which can be computed as

$$P_q^{(i,j)}(e) = \frac{1}{2} erfc \sqrt{\frac{SINR^{(i,j)}}{2}} \qquad (16)$$

For each received symbol, a binary random variable $e_q \in \{0,1\}$ is generated, where the probability of $e_q = 1$ is given by the bit error probability $P_b(e)$ in equation (18) and indicates whether an error occurred during the transmission of the q^{th} bit from user i to user j.

The bit error probability estimation is modified according to the PPM order M, and the symbol error probability is estimated using the union bound approximation

$$P(e) \leq \frac{M-1}{2} erfc \sqrt{\frac{log_2 M}{2} \frac{E_b}{N_0}} \quad (17)$$

where E_b is energy per bit.

Finally, the bit error probability is computed as

$$P_b(e) = \frac{M/2}{M-1} P(e) \quad (18)$$

The error rate of the radio channel is then improved by employing a Forward Error Correcting (FEC) technique. Due to their low complexity, good performance and widespread usage, Bose-Chaudhuri-Hocquenghem (BCH) codes (Benedetto. *et al.,* 1999) are adopted. The code word length, information word length and error correction capability t are chosen to match the packet lengths of the exchanged messages. Moreover, in order to enable the receiver to detect the integrity of messages, an 8-bit cyclic-redundancy-check (CRC) code is added after channel decoding. During one frame transmission (consisting of W coded bits), if the total number of bits in error exceeds the error correction capability of the code, $\sum_{q=0}^{W-1} e_q > t$, then the frame transmission fails.

In order to keep the overall signal bandwidth constant, the pulse duration is fixed at $T_m = 2$ ns, and T_b is kept constant in order to obtain a comparable bit rate.

3. Compressed TH M-Ary PPM

In this section, the proposed TH M-Ary PPM technique is discussed and compared to the conventional one. By examining Figure 3 one more time, it is easily noticed that at the end very narrow N_p pulses of the order of nanoseconds will carry the useful information in each symbol. As those pulses have few nanoseconds duration and naturally could be considered very narrow compared to total symbol duration, there is no real need for extending the total symbol duration when applying higher order PPM modulation (i.e. $T_s = T_b$ for 2PPM, $T_s = 4T_b$ for 16PPM and so on). Taking this simple observation into action; the Compressed TH M-Ary PPM technique (CTH M-Ary PPM) is proposed. In this technique, fixed symbol duration is adopted while moving toward higher order PPM modulation. As a result, the number of TH chips (G) will be reduced, and as those chips are available for each pulse to hop within each frame duration T_f in each symbol, this from one hand will appear to affect the SINR quality at the pulse level. However, on the other hand and for the same amount of data, our proposal reduces the overall time required to complete a transmission from any user compared with the time required while using conventional TH M-Ary PPM. As a consequence, the overall probability of users' collisions is lower, and so, reducing the chance of interference to occur from the beginning on the pulse level.

Figure 4 summarizes the structure of CTH M-Ary PPM and compares it with the conventional scheme as in Figure 3. It can be seen that they are the same regarding the parameters for 2PPM, while for 16PPM modulation the symbol duration (T_s) in the compressed scheme is one-fourth that of the conventional one. So the symbol duration is kept equal to the bit duration while moving toward higher order modulation to reduce the time required transmitting the data and so reducing the collision probability.

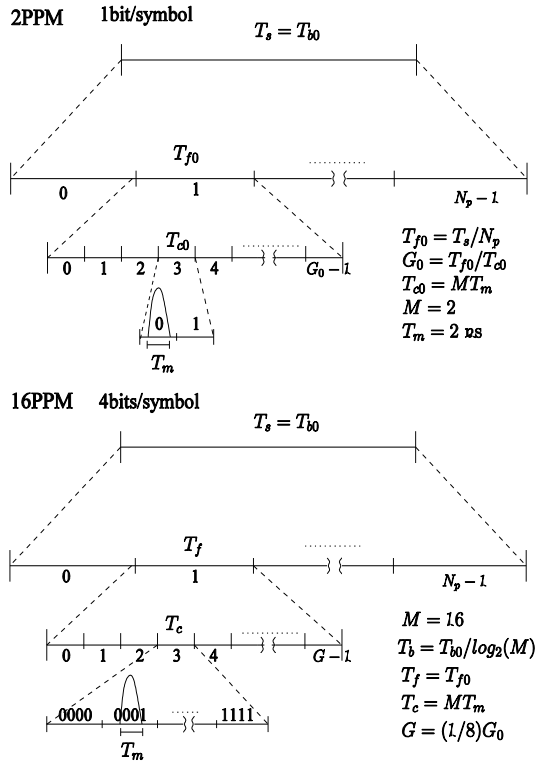

Fig. 4. Symbol structure for the compressed 2-PPM and 16-PPM modulation

4. Performance Evaluation

4.1 Reference scenario

Consider N users in a communications network, using the Aloha access scheme, with a Poisson-distributed arrival rate, λ. Furthermore, an interference-dominated system is adopted, and all users are assumed to be within the same transmission range.

Table 2: Configuration Parameters

Parameters	**TH M-Ary PPM**	**CTH M-Ary PPM**
Modulation order M	2, 4, 8 and 16PPM	
Bit duration T_b	1 μs	
Pulse duration T_m	2 ns	
Chip duration T_c	$M \times T_m$	

Symbol duration T_s	$\log_2 M \times T_b$	T_b
Pulses/Symbol N_p	4	
Frame duration T_f	T_s/N_p	
Number of Chips G	$G = T_f/T_c$	
Bandwidth B	500 MHz	
Poisson arrival rate λ	[0-1]	
Message length	96 bit	
Number of users, N	50	

The configuration parameters for both conventional and compressed TH M-Ary PPM are shown in Table 2. Setting $T_b = 1\ \mu s$, the compression operation up to 16PPM is simulated. To simulate higher order PPM (i.e. 32PPM and more), T_b should be increased in such a way that the compression operation does not exceed the physical limits of such technique.

4.2 Simulations and Results

To carry out simulation and evaluations, a new Omnet++ module is developed in (OMNeT., 2019) to simulate the UWB radio technology. The reference scenario is mentioned in 4.1, and the network setup parameters are described in Table 2. The receiver's noise figure (F) and the link margin (L_M) are chosen to be 6 dB and 5 dB, respectively (Sheng. *et. al.*, 2003). The performance of the proposed scheme is evaluated and then compared with the conventional one.

SEP versus different numbers of users: Figure 5 shows the average Symbol Error Probability (SEP) as a function of the number of users for 2PPM modulation. Both schemes give almost the same performance when the number of users is less than 20. Beyond this number, our scheme outperforms the conventional one.

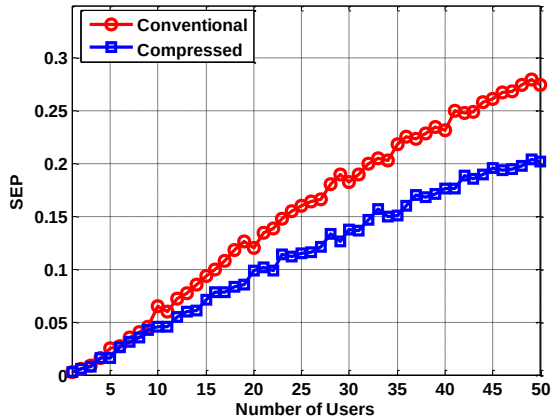

Fig. 5. Performance comparison: 2PPM modulation schemes

As the order of PPM modulation increases, there is a very good enhancement in terms of SEP using the compressed scheme compared to the conventional one. This is due to the short time duration needed by any user for transmitting data in the compressed scheme compared with the conventional scheme. In other words, in the compressed scheme a user may finish transmission while other users have not yet begun to transmit data, while in the conventional scheme, the user takes a longer time to transmit and the probability that other users start transmission while the current user is still transmitting is higher. Respectively, corresponding results are shown in Figure 6 and Figure 7 for 4PPM and 8PPM.

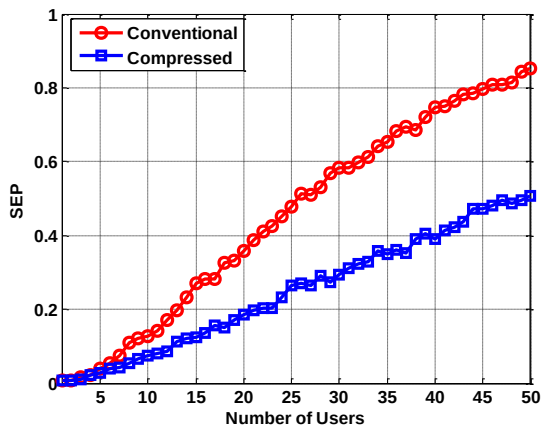

Fig. 6. Performance comparison: 4PPM modulation schemes

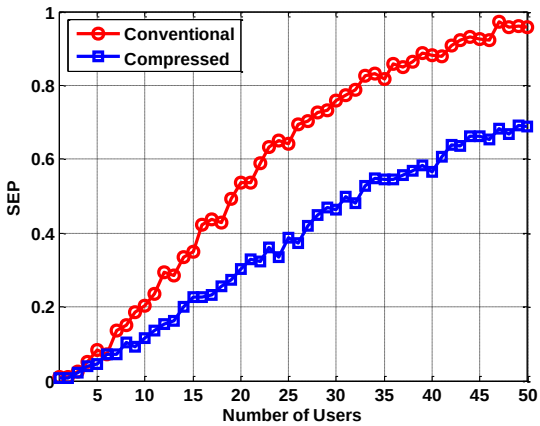

Fig. 7. Performance comparison: 8PPM modulation schemes

Increasing PPM modulation order up to 16PPM while using the compressed scheme will result in decreasing the number of chips G available for each pulse to one-fourth as discussed earlier even though the compressed scheme outperforms the conventional scheme once again, as shown in Figure 8.

Impact of Poisson arrival rate: The Poisson arrival rate parameter λ has also a good influence on the performance of the two schemes; with an increased in arrival rate of users, the probability of interference will also increase.

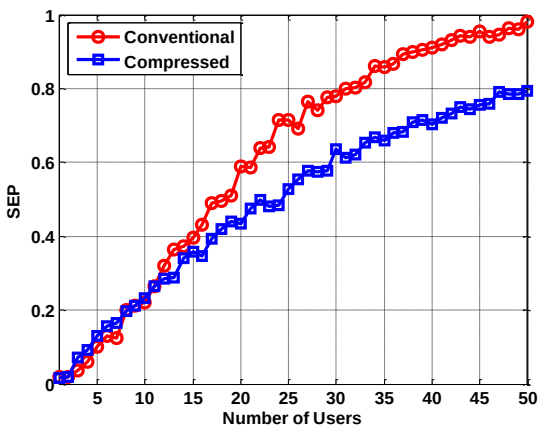

Fig. 8. Performance comparison: 16PPM modulation schemes

The Poisson arrival rate parameter (λ) defines the time between each pair of consecutive transmissions. As the arrival rate of users increases, the probability of interference will also increase. Figures 9, 10 and 11 compare the impact of increasing λ on the probability of error for a fixed number of users (20 users) for both schemes for 4PPM, 8PPM and 16PPM, respectively. As λ increases the interference increases as well in both methods but with less impact on the system performance while using the compressed case.

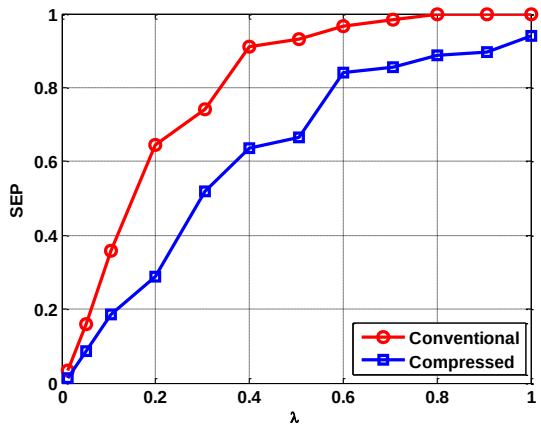

Fig. 9. Performance comparison: 4PPM modulation schemes using different values of λ

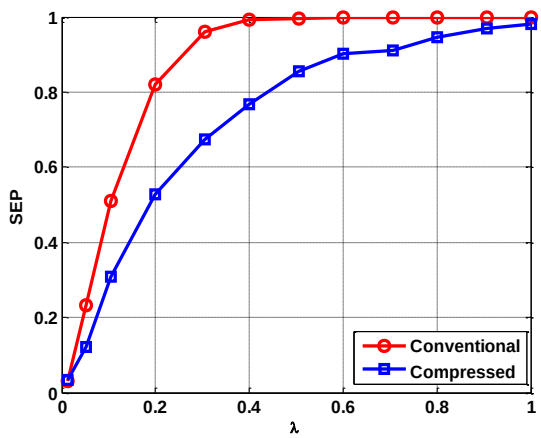

Fig. 10. Performance comparison: 8PPM modulation schemes using different values of λ

As the order of PPM increases, the disparity between both methods is decreased since the transmission time in the conventional method is increased, which results in a greater probability of interference, while in the compressed approach the number of chips is decreased, which result in increasing the pulse collision probability and thus increasing the SEP. However, the compressed approach still outperforms the conventional one.

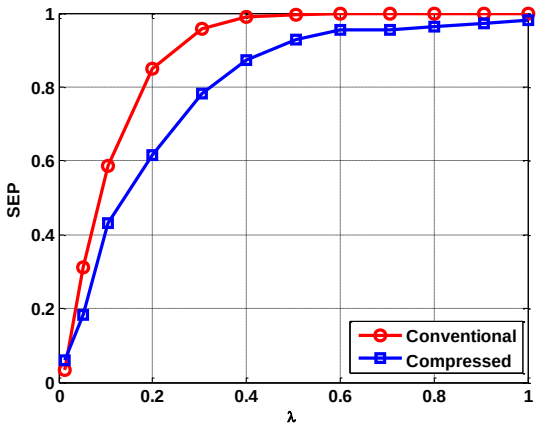

Fig. 11. Performance comparison: 16PPM modulation schemes using different values of λ

5. Conclusion

In this paper, a Compressed TH M-Ary PPM modulation technique for improved performance of UWB radio technology is presented. Moreover, a detailed channel model with SINR derivations is given. In comparison with the conventional TH M-Ary PPM, the proposed scheme saves communication resources and improves quality of service under interference dominated scenarios. Extensive simulation evaluations and results are given to show how the compressed technique enhances the transmission quality in terms of symbol error probability and Poisson arrival rate versus number of users. Finally, the compressed technique is compared with the conventional TH M-Ary PPM.

References

Jain, N., Soni, S., & Bansal, B. (2017). Time-Domain Analysis of Monocycle Pulse Propagation for 5G UWB Communications. *IEEE International Conference on Computing, Communication and Automation (ICCCA2017)*. https://doi.org/10.1109/CCAA.2017.8230054

Nekoogar, F. (2005). Ultra-Wideband Communications: Fundamentals and Applications. *Prentice Hall, New Jersey, 1st Ed*, pp. 32.

Federal Communications Commission. (2002). *Revision of part 15 of the commission's rules regarding Ultra-Wideband transmission systems*. ET Docket No 98-153, Washington, D.C.

Zhang, J., Orlik, P. V., Sahinoglu, Z., Molisch, A. F., & Kinney, P. (2009). UWB Systems for Wireless Sensor Networks. *IEEE Proceedings*. vol. 97, issue 2, pp. 313 – 331. https://doi.org/10.1109/JPROC.2008.2008786

Masri, A., Chiasserini, C. F., Casetti, C., & Perotti, A. (2012). Common control channel allocation in cognitive radio networks through UWB communication. *Journal of Communications and Networks*. vol.14 ,no. 6, pp. 710–718. https://doi.org/10.1109/JCN.2012.00037

Kokkalis, N. V., Mathiopoulos, P. T., Karagiannidis, G. K., & Koukourlis, C. S. (2006). Performance Analysis of M-Ary PPM TH-UWB Systems in the Presence of MUI and Timing Jitter. *Selected Areas in Communications*. vol. 24, no. 4, pp. 822–828. https://doi.org/10.1109/JSAC.2005.863849

Kokkalis, N. V., Takis Mathiopoulos, P., Karagiannidis, G. K., & Koukourlis, C. S. (2008). Capacity performance analysis of M-Ary PPM TH-UWB systems in the presence of narrowband interference. *Journal of Communications and Networks*. vol. 10, no. 3, pp. 297–300. https://doi.org/10.1109/JCN.2008.6388350

Wang, T., & Qi, B. (2014). Analyzing the multiple access performance of ultra wideband time hopping bipolar modulation impulse radio from spectrum point of view. *Proceedings of the IEEE 6th Circuits and Systems*

Symposium. vol. 4, pp. 485–488. https://doi.org/10.1109/CASSET.2004.1321931

Di Benedetto, M. G., Nardis, L., & Giancola, G. (2005). $(UWB)^2$: uncoordinated, wireless, baseborn medium access for UWB communication networks. *Journal of Mobile Networks and Applications*, vol. 10, no. 5, pp. 663-674. https://doi.org/10.1007/s11036-005-3361-z

Shen, Y. S., Ueng, F. B., & Jeng, L. D. (2011). A new time-hopping/direct-sequence biorthogonal PPM UWB communication system. *EURASIP Journal on Wireless Communications and Networking*. vol. 149. https://doi.org/10.1186/1687-1499-2011-149

Masri, A., Chiasserini, C. F., & Perotti, A. (2010). Control information exchange through UWB in cognitive radio networks. *IEEE International Symposium on Wireless Pervasive Computing, (ISWPC)*. pp. 110–115, Modena. https://doi.org/10.1109/ISWPC.2010.5483805

Bai, Z., Xu, S., Zhang, W., & Kwak, K. (2006). A Modified M-Ary TH-PPM Ultra Wideband Communication System. *Asia-Pacific Conference on Communications*. pp. 1-5. https://doi.org/10.1109/APCC.2006.255870

Molisch, A. F., Cassioli, D., Chong, C.-C., Emami, S., Fort, A., & Kannan, B. (2006). A comprehensive standardized model for ultra wideband propagation channels. *IEEE Transactions on Antennas and Propagation*. vol. 54, no. 11, pp. 3151–3166. https://doi.org/10.1109/TAP.2006.883983

Lovelace, W. M., & Townsend, J. K. (2002). The Effects of Timing Jitter and Tracking on the Performance of Impulse Radio. *IEEE Journal*. vol.20,no. 9, pp. 1646–1651. https://doi.org/10.1109/JSAC.2002.805058

Durisi, G., & Benedetto, S. (2003). Performance evaluation of TH-UWB system in the presence of multiuser interference. *IEEE Communication Letters*. vol. 7, no. 5, pp. 224–226. https://doi.org/10.1109/LCOMM.2003.812171

Sheng, H., Orlik, P., Haimovich, A. M., Cimini, A. M., & Zhang, J. (2003). On the spectral and power requirements for ultra-wideband transmission. *IEEE ICC*. vol. 1, pp. 738–742. https://doi.org/10.1109/ICC.2003.1204271

Saleh, A. A. M., & Valenzuela, R. A. (1987). A statistical model for indoor multipath propagation. *IEEE Journal on Selected Areas In Communications*. vol. SAC-5, no. 2, pp. 128–137. https://doi.org/10.1109/JSAC.1987.1146527

Benedetto, S. & Biglieri, E. (1999). Principles of digital transmission with wireless applications. *New York: Plenum/Kluwer Publishers*.

OMNeT++. (2019). https://omnetpp.org/